ELSEVIER

Chemical Engineering Journal 138 (2008) 442–451

Chemical Engineering Journal

www.elsevier.com/locate/cej

The effect of heat-flux profile and of other geometric and operating variables in designing industrial membrane methane steam reformers

M. De Falco [a,*], P. Nardella [a], L. Marrelli [a], L. Di Paola [a], A. Basile [b], F. Gallucci [b]

[a] *Chemical Engineering Department, University of Rome "La Sapienza", Via Eudossiana 18, 00184 Roma, Italy*

[b] *Institute on Membrane Technology, ITM-CNR, c/o University of Calabria, Via P. Bucci, cubo 17/C, I-87030 Rende (CS), Italy*

Received 26 February 2007; received in revised form 22 June 2007; accepted 25 June 2007

Abstract

The performance of an original membrane methane reformer is analyzed by a two-dimensional mathematical model. The reactor is a bundle of four coaxial double tubes inserted in a shell in which a heating fluid flows. The annular region of each tube is the reaction zone, whereas the inner tube is the selective membrane for hydrogen removal. Many simulations have been carried out in order to find a suitable set of values of geometric and operating design variables. The effect of pressure and sweeping gas flow rate at permeation side, of membrane diameter and of axial profile of heat flux supplied to the reactor is analyzed in 81 virtual experiments. Suitable operating conditions are found: over 58% methane conversion can be reached, within a proper membrane temperature range and extra methane consumption for thermal duty.
© 2007 Elsevier B.V. All rights reserved.

Keywords: Methane steam reforming; Membrane reactor; Hydrogen production; Design variables

1. Introduction

The demand of hydrogen in refineries has increased more and more in the last years and it's foreseeable that in the next future deteriorating quality of crude oils, more stringent petroleum product specifications and environmental problems will lead to larger need of hydrogen to use in hydroprocessing processes. Moreover, the development of fuel cell technology and its application in many fields will contribute to increase requirements of pure hydrogen.

This market evolution is stimulating the development of new technologies to produce a large amount of hydrogen at low cost. Currently, the most promising process is based on the integration of selective membranes in steam reforming reactors in order to continuously remove hydrogen from reaction environment. Quite high methane conversions at relatively low temperatures can be obtained in such a way and very pure hydrogen is collected in the permeation zone.

The methane steam reforming process is based on the following main reactions:

$$CH_4 + H_2O \Leftrightarrow CO + 3H_2 \qquad \Delta H^0_{298} = 206\,\text{kJ/mol} \qquad (1)$$

$$CO + H_2O \Leftrightarrow CO_2 + H_2 \qquad \Delta H^0_{298} = -41\,\text{kJ/mol} \qquad (2)$$

which, taken together, yield:

$$CH_4 + 2H_2O \Leftrightarrow CO_2 + 4H_2 \qquad \Delta H^0_{298} = 165\,\text{kJ/mol} \qquad (3)$$

The process is highly endothermic and very fast over Ni/Al_2O_3 catalyst. Equilibrium condition threshold compels to operate at high temperature and tubular packed bed reactors are usually placed in a furnace where the heat produced by combustion is transferred to the process through the reformer tube walls. In such a configuration, reformer tubes are subjected to large stresses due to high operating temperatures with large gradients in axial and radial directions, up to the point that the high pressure inside the tube could provoke creep rupture. Moreover, a great amount of methane has to be burned to supply the high heat flux required by reactions.

The integration into the reactor of Pd-based membranes, extremely selective towards hydrogen, allows a lower temperature operation, since the removal of a reaction product prevents the equilibrium to be achieved. Therefore, other methods than methane combustion in a furnace could be used to supply the heat required by reforming reactions.

Several papers concerning the use of membrane reactors in steam reforming have appeared in the literature [1–7] but almost all these works deal with small scale reformers and very long

* Corresponding author. Tel.: +39 0347 6809041.
E-mail address: marcello.defalco@uniroma1.it (M. De Falco).

1385-8947/$ – see front matter © 2007 Elsevier B.V. All rights reserved.
doi:10.1016/j.cej.2007.06.026

Nomenclature

B_H	hydrogen permeability (kmol m^{-1} h^{-1} kPa^{-05})
c_i	molar concentration (kmol m^{-3}), i = CH_4, H_2O, H_2, CO, CO_2
c_i^{in}	inlet molar concentration (kmol m^{-3}) i = CH_4, H_2O, H_2, CO, CO_2
$c_{p,m}$	gas mixture specific heat (kJ kmol^{-1} K^{-1})
$c_{p,perm}$	gas mixture specific heat in permeation zone (kJ kmol^{-1} K^{-1})
c_{tot}	total concentration (kmol m^{-3})
d_p	equivalent particle diameter (m)
f	friction factor
$F_{CH_4}^{in}$	inlet methane flow rate (kmol h^{-1})
$F_{CH_4}^{out}$	outlet methane flow rate (kmol h^{-1})
$F_{CO_2}^{in}$	inlet carbon dioxide flow rate (kmol h^{-1})
$F_{CO_2}^{out}$	outlet carbon dioxide flow rate (kmol h^{-1})
$F_{H_2}^{perm,out}$	outlet hydrogen flow rate in permeation zone (kmol h^{-1})
$F_{p,tot}$	total molar flow rate in permeation zone (kmol h^{-1})
F_{sweep}	sweeping gas flow rate in permeation zone (kmol h^{-1})
G	mass specific gas flowrate (kg m^{-2} h^{-1})
h_{P,H_2}	permeation zone hydrogen enthalpy (kJ kmol^{-1})
h_{R,H_2}	reaction zone hydrogen enthalpy (kJ kmol^{-1})
h_w	heat transport coefficient near wall (kJ m^{-2} h^{-1} K^{-1})
$h_{w,p}$	heat convective transport coefficient in permeation zone (kJ m^{-2} h^{-1} K^{-1})
$(-\Delta H_j)$	j-th reaction enthalpy (kJ mol^{-1})
L	reactor length (m)
$N_{H_2}^m$	hydrogen flux permeating through membrane (kmol m^{-2} h^{-1})
p	emissivity of solid surface
$p_{H_2,perm}$	hydrogen partial pressure in permeation zone (kPa)
$p_{H_2,reac}$	hydrogen partial pressure in reaction zone(kPa)
Pe_{mr}	mass effective radial Peclet number
P_P	permeation zone pressure (kPa)
P_P^{in}	inlet permeation zone pressure (kPa)
P_R	reaction zone pressure (kPa)
P_R^{in}	inlet reaction zone pressure (kPa)
Pr	Prandtl number
q_m	heat flux from the reaction to the permeation zone (kW m^{-2})
q_r	heat flux from outside to the reaction zone (kW m^2)
$\tilde{r}$	dimensionless radial coordinate
$r_{i,i}$	inner tube internal radius (m)
$r_{o,i}$	inner tube external radius (m)
$r_{i,o}$	outer tube internal radius (m)
$r_{o,o}$	outer tube external radius (m)
R	gas universal constant (kJ kmol^{-1} K^{-1})
R_j	kinetic rate of j-th reaction (kmol kg$_{cat}^{-1}$ h^{-1})
Re	Reynolds number
T_{mem}	membrane temperature (K)
$T_{mem,max}$	maximum membrane temperature (K)
T_p	permeation zone temperature (K)
T_p^{in}	inlet permeation zone temperature (K)
T_R	reaction zone temperature (K)
T_R^{in}	inlet reaction zone temperature (K)
$T_{w,o}$	external wall temperature (K)
u_z	gas velocity (m h^{-1})
u_z^{in}	inlet gas velocity (m h^{-1})
U	overall heat transfer coefficient (outside-reaction zone) (kJ m^{-2} h^{-1} K^{-1})
U_1	overall heat transfer coefficient (reaction–permeation zone) (kJ m^{-2} h^{-1} K^{-1})
X_{CH_4}	methane conversion
X_{CO_2}	carbon dioxide yield
Y_{H_2}	hydrogen recovered per mole of methane
z	dimensionless axial coordinate

Greek symbols

α_{mem}	membrane thermal conductivity (kJ m^{-2} h^{-1} K^{-1})
α_{met}	metal thermal conductivity (kJ m^{-2} h^{-1} K^{-1})
α_{ru}, α_{rs}	parameters defined by Eq. (18) (kJ m^{-2} h^{-1} K^{-1})
δ	membrane thickness (m)
ϵ	void fraction
η_j	effectiveness factor of the j-th reaction
λ_{er}	effective radial thermal conductivity (kJ m^{-1} h^{-1} K^{-1})
λ_{er}^0	static radial thermal conductivity (kJ m^{-1} h^{-1} K^{-1})
λ_g	gas phase thermal conductivity (kJ m^{-1} h^{-1} K^{-1})
λ_S	packing material thermal conductivity (kJ m^{-1} h^{-1} K^{-1})
μ_g	gas mixture viscosity (kg m^{-1} h^{-1})
ρ_b	packed bed density (kg m^{-3})
ρ_g	gas mixture density (kg m^{-3})

residence times of gas mixture in the reaction environment. Only few studies face the industrial application of membrane reactor technology: Fernandez and Soares Jr. [8] have simulated a large scale membrane reactor by using an one-dimensional model; Koukou et al. [9] and Basile et al. [10] have studied the behaviour of a ceramic membrane reactor and a dense Pd–Ag membrane reactor, respectively, for water gas shift reaction (Eq. (2)) by a two-dimensional model; Fukuhara and Igarashi [11] have used a two-dimensional model to simulate a membrane reactor for dehydrogenation of ethylbenzene.

Recently, De Falco et al. [12] have compared the performance of a steam reforming membrane reactor (MR) and of a traditional reactor (TR), both operating at industrial conditions: a geometric configuration (length = 12 m, diameter = 0.12 m) was assumed and the same operating conditions have been fixed for

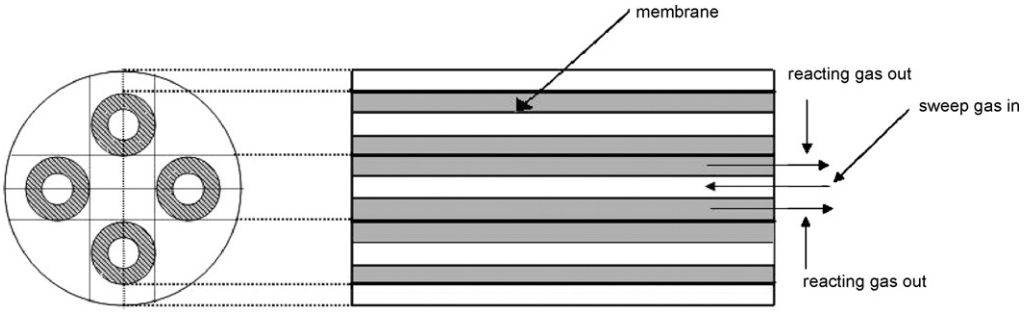

Fig. 1. Membrane reformer configuration.

both the reformers. On the other hand, membrane reactor performance may be improved at different geometries and operating conditions.

The aim of this work is to analyze the behaviour of a membrane reactor designed in an original configuration which should allow the use of a heat supply system (like molten salts) different from the furnace traditionally used in steam reforming. The joint effect of four operating variables and geometric parameters is simulated by means of a two-dimensional model. A good set of parameters is found and benefits and drawbacks are analyzed in comparison with the traditional configuration.

The configuration considered in simulations is a bundle of four coaxial double tubes inserted in a shell in which a heating fluid flows (Fig. 1). The annular zone of each double tube is the reaction zone where catalytic pellets at relatively high temperature are packed out [13]; the internal tube is the selective membrane where a sweeping gas (water vapour) is sent counter-current. The membrane is assumed to be a Pd-based thin layer, supported on a ceramic or metallic material.

The four design variables, selected among many others affecting process performance, are:

(1) The membrane tube external radius $r_{o,i}$;
(2) The permeation zone pressure P_p;
(3) The sweeping gas flow rate in each tube F_{sweep};
(4) The slope A of axial profile, assumed to be linear, of heat flux supplied by a heating fluid flowing in the external shell.

Other operating variables and geometric parameters have been fixed on the basis of typical industrial conditions.

2. Mathematical model

The mathematical model is based on mass, energy and momentum balances in reaction and permeation zone, with the following assumptions:

- Only reactions (1–3) are considered (secondary reactions are neglected).
- Steady-state conditions.
- Negligible axial dispersion and radial convective terms.
- Ideal gas behaviour.
- Each double tube is representative of any other tube.
- Pseudo-homogenous condition inside the reactor.
- Permselectivity of Pd-based membrane towards hydrogen 100%.
- The influence of the membrane support on the heat and mass transfer is negligible.

In the annular reaction zone, a two-dimensional, non-isothermal and non isobaric model is used to calculate axial and radial profile of concentrations and temperature; in the permeation, zone isobaric conditions are assumed, and a one-dimensional model is applied.

Equations of the MR model, together with boundary conditions, are:

- Mass balances:
  - Reaction zone: $i = CH_4, H_2O, H_2, CO, CO_2$:

$$\frac{\partial(u_z c_i)}{\partial \tilde{z}} = \frac{d_P L}{Pe_{mr} r_{i,o}^2}\left(\frac{\partial^2(u_z c_i)}{\partial \tilde{r}^2} + \frac{1}{\tilde{r}}\frac{\partial(u_z c_i)}{\partial \tilde{r}}\right) + \rho_b L \sum_j \eta_j R_j \tag{4}$$

  - Permeation zone:

$$\frac{dY_{H_2}}{d\tilde{z}} = -\frac{N_{H_2}^m 2\pi r_{o,i}}{F_{CH_4}^{in}} \tag{5}$$

The sign — means relates to the counter-current configuration.

- Energy balances
  - Reaction zone:

$$\frac{\partial T_R}{\partial \tilde{z}} = \frac{\lambda_{er} L}{(u_z c_{tot}) c_{p,m} r_{i,o}^2}\left(\frac{\partial^2 T_R}{\partial \tilde{r}^2} + \frac{1}{\tilde{r}}\frac{\partial T_R}{\partial \tilde{r}}\right) + \frac{\rho_b L \sum_j \eta_j (-\Delta H_j) R_j}{(u_z c_{tot}) c_{p,m}} \tag{6}$$

  - Permeation zone:

$$\frac{dT_P}{d\tilde{z}} = \frac{L}{F_{P,tot} c_{p,perm}}(U_1 2\pi r_{i,i}(T_R - T_P) + N_{H_2}^m \pi r_{o,i}(h_{R,H_2} - h_{P,H_2})) \tag{7}$$

- Momentum balance
  - Reaction zone:

$$\frac{dP_R}{d\tilde{z}} = -\frac{fG\mu_g L}{\rho_g d_P^2}\frac{(1-\epsilon)^2}{\epsilon^3} \tag{8}$$

where the friction factor is calculated by the well-known Ergun model:

$$f = 150 + 1.75\frac{Re}{1-\epsilon} \tag{9}$$

- Boundary conditions

$$\tilde{z} = 0, \vee\tilde{r} \rightarrow \begin{cases} u_z c_i = u_z^{\text{in}} c_i^{\text{in}} \\ T_R = T_R^{\text{in}} \\ P_R = P_R^{\text{in}} \end{cases} \tag{10}$$

$$\tilde{z} = 1, \vee\tilde{r} \rightarrow \begin{cases} Y_{H_2} = 0 \\ T_P = T_P^{\text{in}} \end{cases} \tag{11}$$

$$\tilde{r} = \tilde{r}_{i,o}, \vee\tilde{z} \rightarrow \begin{cases} \dfrac{\partial(u_z c_i)}{\partial\tilde{r}} = 0 \\ \lambda_{er}\dfrac{\partial T_R}{\partial\tilde{r}} = q_r = U(T_{w,o} - T_{R|r_{i,o}}) \end{cases} \tag{12}$$

$$\tilde{r} = \tilde{r}_{o,i}, \vee\tilde{z} \rightarrow \begin{cases} \dfrac{\partial(u_z c_i)}{\partial\tilde{r}} = 0 \\ \dfrac{d_p}{Pe_{mr}}\dfrac{\partial(u_z c_{H_2})}{\partial\tilde{r}} = N_{H_2}^m \\ \lambda_{er}\dfrac{\partial T_R}{\partial\tilde{r}} = q_m = U_1(T_{R|r_{o,i}} - T_P) \end{cases} \tag{13}$$

In Eq. (4), the mass effective radial Peclet number is Pe_{mr}, calculated by the expression reported by Kulkarni and Doraiswamy [14] and valid for $Re > 1000$; η_j and R_j are, respectively, the effectiveness factor and the rate of the j-th reaction, calculated by Xu and Froment expressions [15].

In Eq. (5), Y_{H_2} is the hydrogen recovered per mole of inlet methane and $N_{H_2}^m$ is the hydrogen flux permeating through the membrane:

$$N_{H_2}^m = \frac{B_H}{\delta}(p_{H_2,reac}^{0.5} - p_{H_2,perm}^{0.5}) \tag{14}$$

Eq. (14) is the Sievert law, suitable for thick dense membrane, i.e. in the case of limiting diffusion of atomic hydrogen in the metallic layer; δ is the Pd-based membrane thickness (20 μm in our simulations), $p_{H_2,reac}$ and $p_{H_2,perm}$ are hydrogen partial pressures in the reaction and permeation zone, respectively, and B_H is the membrane permeability, which depends on temperature and membrane composition. Shu's expression of B_H [1] for Pd–Ag (5.1 wt%) membranes is used in this work:

$$B_H = 7.928 \times 10^{-5}\exp\left(-\frac{15,700}{RT_{mem}}\right) \tag{15}$$

The membrane support is a porous seamless 316 L stainless steel with a nominal particle retention size of 0.2 μm, which is a dimension much higher than molecular diameters of the components. Therefore the effect on the mass transport resistance of the porous media is negligible in respect to the resistance of the Pd-based alloy layer, in which a solution-diffusion mechanism occurs. Moreover the stainless steel is characterized by a high heat transport conductivity and consequently its influence on the global heat transfer conductivity between reaction and permeation zone is assumed to be negligible as well.

In Eq. (6), $(-\Delta H_j)$ is the j-th reaction enthalpy and λ_{er} is the effective radial thermal conductivity of packed bed and gas mixture taken as a pseudo-homogeneous phase. λ_{er} is calculated by the following expression [16]:

$$\lambda_{er} = \lambda_{er}^0 + 0.111\lambda_g\frac{Re_p Pr^{1/3}}{1 + 46(d_p/2r_{i,o})^2} \tag{16}$$

where the static contribution λ_{er}^0 is given by:

$$\lambda_{er}^0 = \epsilon(\lambda_g + 0.95\alpha_{ru}d_p) + \frac{0.95(1-\epsilon)}{2/3\lambda_s + 1/(10\lambda_g + \alpha_{rs}d_p)} \tag{17}$$

and:

$$\alpha_{ru} = \frac{0.8171(T/100)^3}{1 + \epsilon/2.(1-\epsilon)(1 - p/p)}$$

$$\alpha_{rs} = 0.8171\left(\frac{p}{2-p}\right)(T/100)^3 \tag{18}$$

The overall heat transfer coefficient U (Eq. (12)) between outside and the reaction zone is expressed as:

$$U = \left(\frac{1}{h_w} + \frac{1}{\alpha_{met}}\right)^{-1} \tag{19}$$

where α_{met} is the metal tube conductivity and h_w is the heat transfer coefficient of an "unmixed layer" near the tube wall where heat transport occurs only by molecular conduction [17]. Different correlations are proposed in the literature to calculate h_w value [18–22]; in the present work Li and Finlayson's [23] expression is used:

$$h_w = 0.17\frac{\lambda_g}{d_p}\left(\frac{Pr}{0.7}\right)^{1/3} Re^{0.79} \tag{20}$$

The overall heat transfer coefficient U_1 (Eqs. (7) and (13)) between reaction and permeation zone is given by:

$$U_1 = \left[\frac{1}{h_w} + \frac{\delta}{\alpha_{mem}} + \frac{r_{o,i}}{r_{i,i}}\frac{1}{h_{w,p}}\right]^{-1} \tag{21}$$

where α_{mem} is the membrane thermal conductivity and $h_{w,p}$ is the heat convective transport coefficient in the permeation zone, calculated in turbulent regime.

2.1. Design variables and simulations

Three possible values are taken for each independent variable (Table 1); therefore, 81 simulations (3^4) are carried out, considering every possible set.

Table 1
Independent variable values for the simulation design

	1	2	3
$r_{o,i}$	0.05	0.06	0.07
F_{sweep}	12	24	36
P_p	101	303	505
A	−10	0	10

Table 2
Operating and geometric parameters

$r_{o,o}$	$r_{i,o}$	$r_{i,i}$	L	
0.1016	0.0916	0.04/0.05/0.06	4.04/4.97/6.82	
P_R^{in}	T_R^{in}	T_P^{in}	$F_{CH_4}^{in}$	S/C
1010	773	773	4	3
$\bar{q}_r$	β			
40	45/40/35			

Table 3
Inlet gas composition [24]

y_{CH_4}	y_{H_2O}	y_{H_2}	y_{CO}	y_{CO_2}
0.228	0.728	0.028	0.008	0.002

Other operating and geometric parameters have been fixed (Tables 2 and 3), according to typical industrial parameters.

Reaction zone pressure (10 bar) is lower than those typically used in industrial reformers (25–30 bar), but thermodynamically more suitable. The overall inlet methane flow rate (16 kmol/h) is distributed into the four parallel reactors such as 4 kmol/h flows in each tube; this value is twice the typical flow rate in a traditional industrial reformer [25]. As for other components, inlet stream composition is taken from [24].

Shell diameter and other geometric dimensions of tubular reactors and membrane are reported in Table 2 and sketched in Fig. 2.

The reformer length is calculated in order to set the catalyst mass per mole of inlet methane to the same value of typical traditional reformers (internal tube diameter 0.126 m, length 12 m, void bed fraction $\epsilon \simeq 0.5$). With the same ϵ, the reformer lengths calculated in the three cases analyzed (Table 1) are 4.04, 4.97, 6.82 m, respectively.

The heat flux axial profile is assumed to be linear:

$$q_r = A\tilde{z} + \beta \tag{22}$$

and a mean value of $q = 40\,\text{kW/m}^2$, which is about half of a typical heat flux value for traditional reformers [26]. Therefore, β is derived from the relation:

$$\beta = 40 - \frac{A}{2} \tag{23}$$

Values of slope A explored in simulations are reported in Table 1: negative and positive A values (cases 1 and 3 in Table 1) mean that heat flux is decreasing or increasing, respectively, along the reactor, whereas $A = 0$ (case 2) indicates a heat flux constant.

Heat flux profiles with $A < 0$, $A \approx 0$ or $A > 0$ could be approximately obtained by arranging co-current or counter-current schemes, flow-rates and thermal properties of heating fluid. For example, cases $A < 0$ and $A \approx 0$ could be approximately obtained by co-current and counter-current mode of reacting mixture and heating fluid, respectively, because of decreasing or constant temperature differences (driving force) along the axis of the

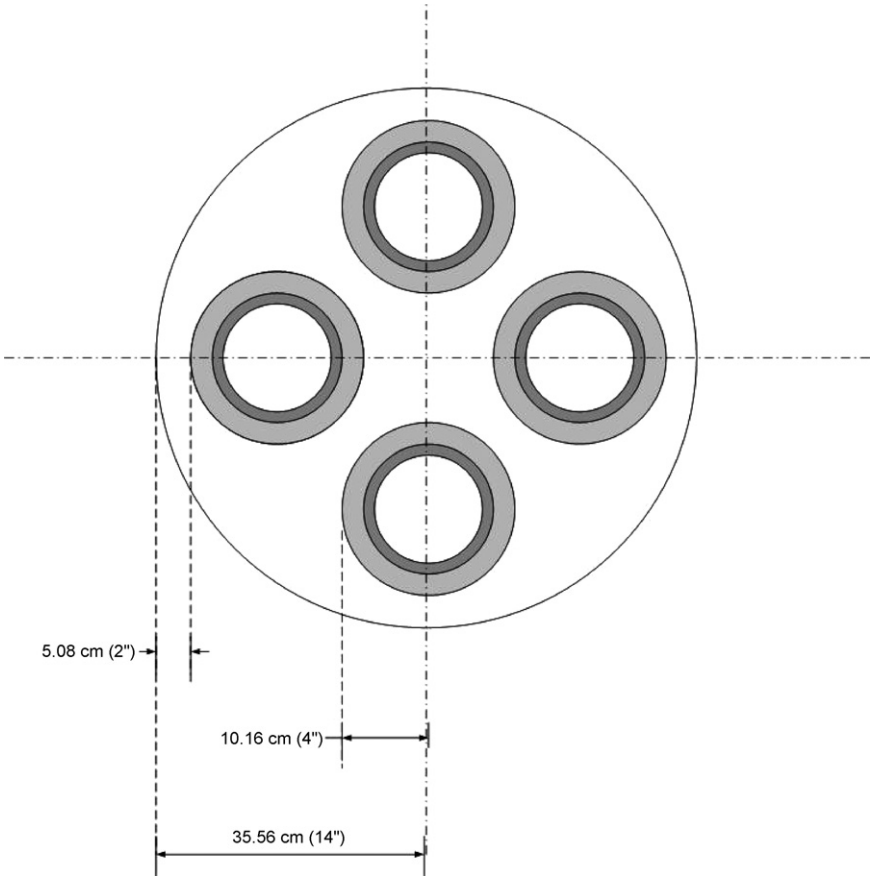

Fig. 2. Membrane reformer configuration section.

reactor. The case $A > 0$ could be obtained by a counter-current scheme with a heating fluid with a low specific heat that exhibits a large temperature drop from exit to inlet section of the reactor.

2.2. Numerical solution

In order to solve the system of partial differential equations, the radial coordinate is discretized by means of central second-order differences: a boundary-value-problem system of first order ordinary differential equations is obtained and solved by a shooting method.

Reactor performance is evaluated through the following quantities:

$$X_{CH_4} = \frac{F^{in}_{CH_4} - F^{out}_{CH_4}}{F^{in}_{CH_4}}$$

methane conversion

$$X_{CO_2} = \frac{F^{out}_{CO_2} - F^{in}_{CO_2}}{F^{in}_{CH_4}}$$

carbon dioxide yield

$$Y_{H_2} = \frac{F^{out}_{H_2,perm}}{F^{in}_{CH_4}}$$

hydrogen recovered per mole of methane.

Moreover, it has been checked if the maximum membrane temperature $T_{mem,max}$ was always lower than 800–815 K; indeed, the Pd-based composite membranes are characterized by a remarkable thermal instability, due to loss of adherence between active principle and support.

3. Results and discussion

Eighty-one simulations have been performed by means of the variables indicated in Table 1. Methane conversion, carbon dioxide yield, hydrogen recovered per mole of methane and maximum membrane temperature have been evaluated in each simulation. The effect of the independent variables has been analyzed and a suitable solution is proposed.

3.1. Effect of the membrane external radius

The membrane tube radius has a large effect on the reformer performance. Fig. 3 shows the dependence of methane conversion and carbon dioxide yield on $r_{o,i}$. Obviously, a large membrane radius involves a high (membrane surface)/(reaction volume) ratio and, consequently, a large hydrogen flow removed from the reaction environment. In fact, Y_{H_2} value is 0.74, 1.13 and 1.82 when $r_{o,i}$ is 0.05, 0.06 and 0.07 m, respectively.

On the other hand, the larger the radius, the closer the membrane to the hot wall and, therefore, the higher the membrane temperature (811.2, 827.9, 855.8 K for $r_{o,i} = 0.05, 0.06, 0.07$ m). Fig. 4 shows the radial temperature profile calculated in the outlet section ($\tilde{z} = 1$) : $\tilde{r} = 0$ is the gas layer near the Pd-based membrane, while $\tilde{r} = 1$ is the gas layer near the hot tube. It has to be noticed that the temperature reached imposing $r_{o,i} = 0.07$ m is too high compared with the current membrane thermal instability threshold.

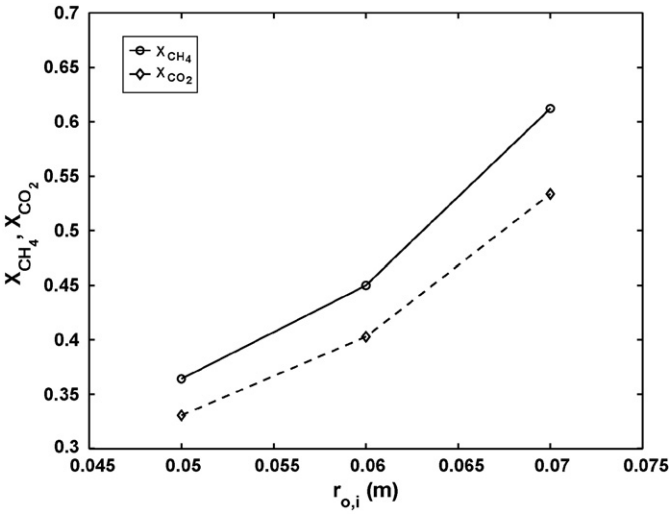

Fig. 3. Methane conversion and carbon dioxide yield vs. membrane tube radius ($F_{sweep} = 24$ kmol/h, $P_p = 303$ kPa, $A = 0$ kW/m^3).

3.2. Effect of the sweeping gas flow rate

The effect of sweeping water vapour flow rate F_{sweep} on X_{CH_4} and X_{CO_2} is negligible (Fig. 5): only a very slight positive effect on conversion appears from simulations, due to the $p_{H_2,perm}$ reduction, that improves the permeating hydrogen flux.

The most important effect of sweeping gas flow rate is the remarkable reduction of maximum membrane temperature ($T_{mem,max} = 842.5$, 827.9, 819.8 K with $F_{sweep} = 12$, 24, 36 kmol/h). The flow of relatively cool sweeping vapour allows the membrane to be maintained at a moderate thermal level, with significant advantages in its life durability and stability. On the other hand, too high water vapour flow rates (such as 36 kmol/h per tube) do not seem to be economically advantageous, since the vapour has to be generated and heated. From now on, an anal-

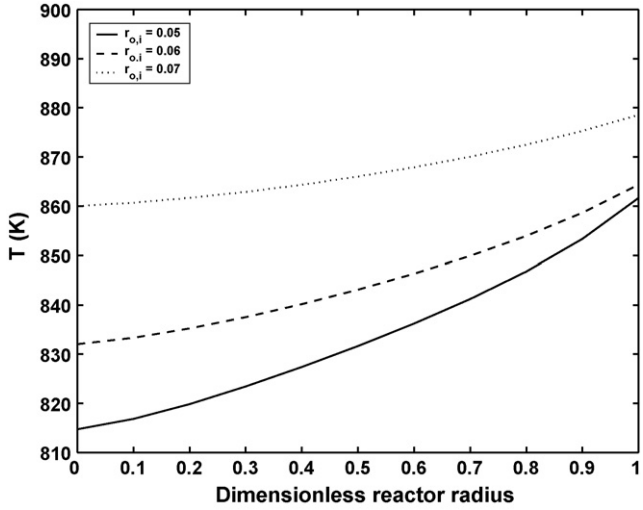

Fig. 4. Radial profiles of temperature at outlet section of the reactor.

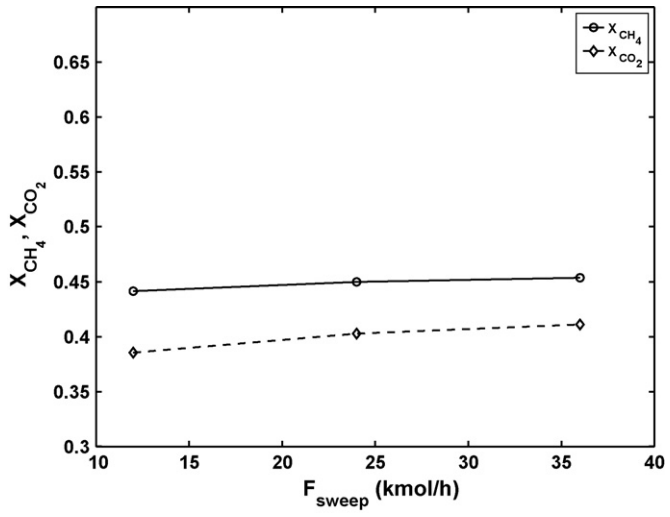

Fig. 5. Methane conversion and carbon dioxide yield vs. sweeping flow ($r_{o,i}$ = 0.06 m, P_p = 303 kPa, A = 0 kW/m^3).

ysis of the steam production cost is carried out and an optimal sweeping gas flow rate is proposed.

3.3. Effect of permeation zone pressure

As reported in the literature [12,27], the reaction zone pressure has a double effect: it improves the permeation flux, by increasing $p_{H_2,reac}$, but, at the same time, it is thermodynamically unfavourable to equilibrium conversion. At high spatial velocity (as assumed in our simulations), the two opposite effects offset each other and the global effect is about inappreciable.

On the other hand, the permeation zone pressure has a significant effect on the reformer performance: its reduction increases the permeation flux and the conversion improves (Fig. 6). Moreover, the larger heat amount required to get higher conversion reduces the reaction temperature and, consequently, the membrane temperature ($T_{mem,max}$ = 818.9, 827.9, 834 K with P_p = 101, 303, 505 kPa). Therefore, reducing permeation zone pressure at the lowest possible value appears to be a very good solution if recompression of H2 is not required for specific uses.

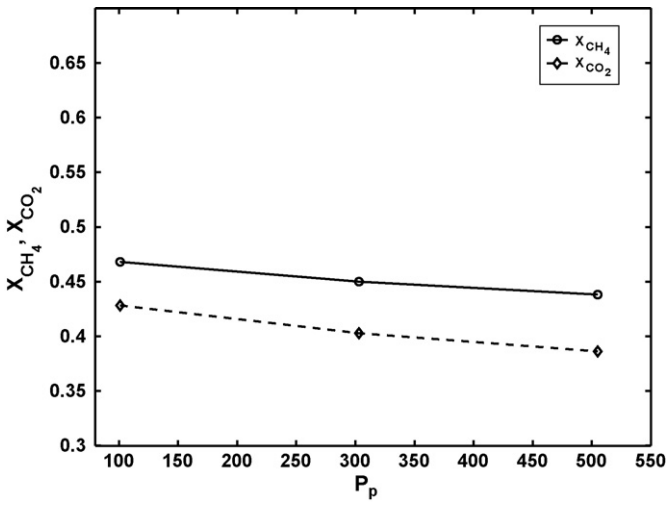

Fig. 6. Methane conversion and carbon dioxide yield vs. permeation zone pressure ($r_{o,i}$ = 0.06 m, F_{sweep} = 24 kmol/h, A = 0 kW/m^3).

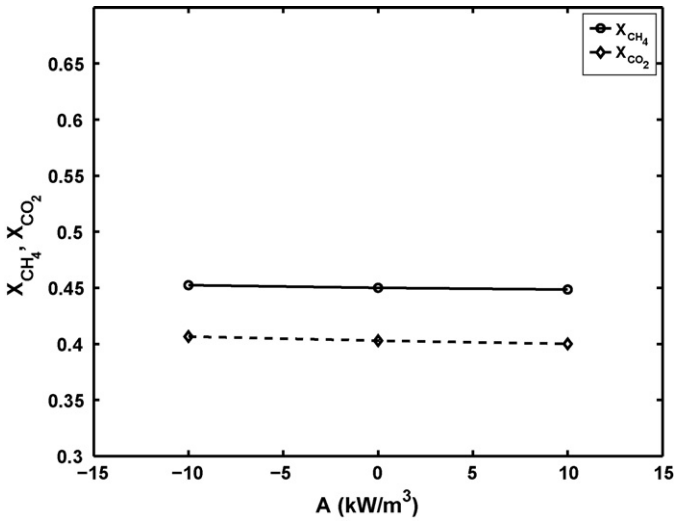

Fig. 7. Methane conversion and carbon dioxide yield vs. heat flux slope ($r_{o,i}$ = 0.06 m, F_{sweep} = 24 kmol/h, P_p = 303 kPa).

3.4. Effect of heat flux

The effect of axial heat profile slope A is shown in Figs. 7–9. A quite negligible influence of A on methane conversion and carbon dioxide yield can be observed (Fig. 7), whereas the maximum membrane temperature decreases favourably at negative slopes of axial heat flux profile (Fig. 8). Fig. 9 shows the effect of A on Y_{H_2}. For $A < 0$, the higher heat flux in the inlet section yields a higher conversion in the first part of the reactor and an increase of hydrogen partial pressure and permeated hydrogen flux which, in its turn, promotes the reaction advancement. Therefore, if a heating fluid is used to supply the heat requested, probably it's advisable sending it in co-current. Finally, the effect of the average thermal flux $q_{r,av}$ on the methane conversion is reported in Fig. 10 for the three different values of membrane

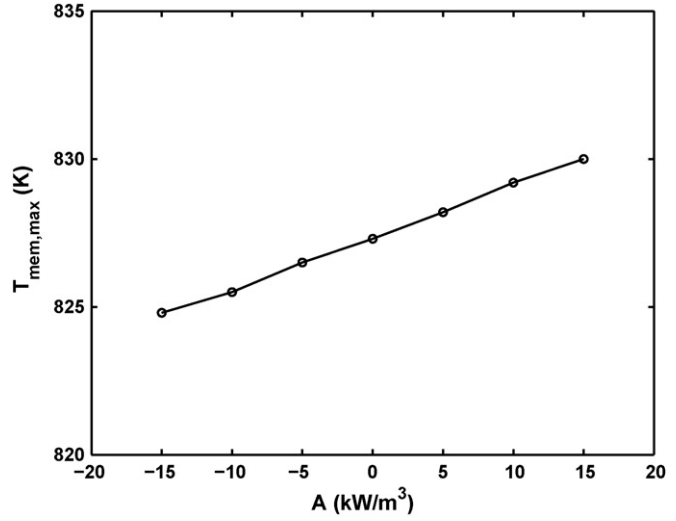

Fig. 8. Maximum membrane temperature for different axial heat flux profiles.

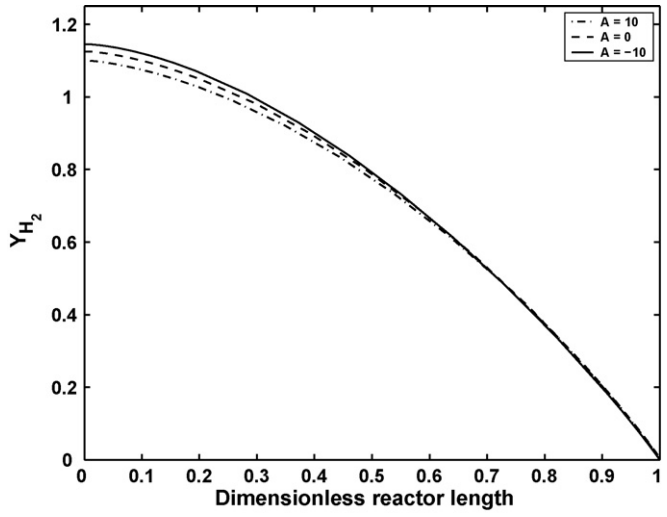

Fig. 9. Hydrogen recovered per mole of methane with different axial heat flux profiles.

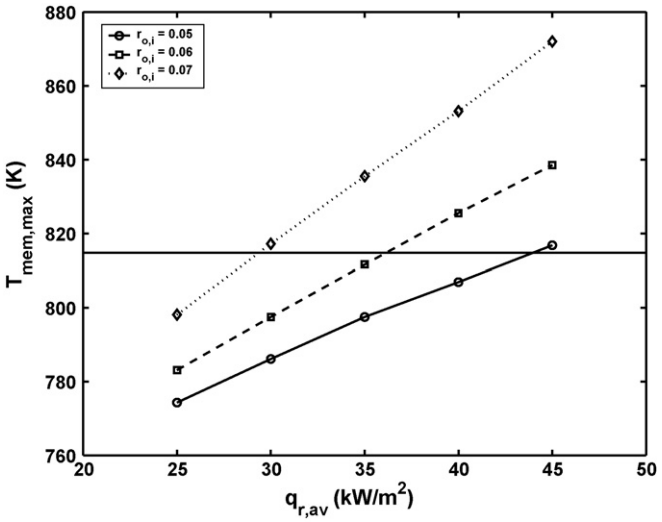

Fig. 11. Effect of the heat flux and membrane tube radius on maximum membrane temperature.

tube radius. Methane conversion increases with $q_{r,av}$ and $r_{o,i}$, but the membrane temperature increases as well, so that its maximum value can overcome somewhere the maximum temperature allowed for membrane stability (see Fig. 11, where the critical value of the temperature is set at 815 K). Obviously, the heat flux supplied has to be restricted to a lower value imposing a greater membrane tube radius.

3.5. Proposed configuration

The main results arising from simulations are:

- The increment of the membrane external radius has a strong positive effect on reformer performance, but it increases the membrane temperature towards unsuitable values;
- Increasing values of sweeping gas flow rate and reducing those of the permeation zone pressure have a slight positive effect on reactor conversion. Very high water vapour flow rates at 773 K in the permeation zone reduce the membrane temperatures, but they introduce large additional cost.
- Supplying heat flux with a negative sloped profile allows the heat to be exploited in a better way.

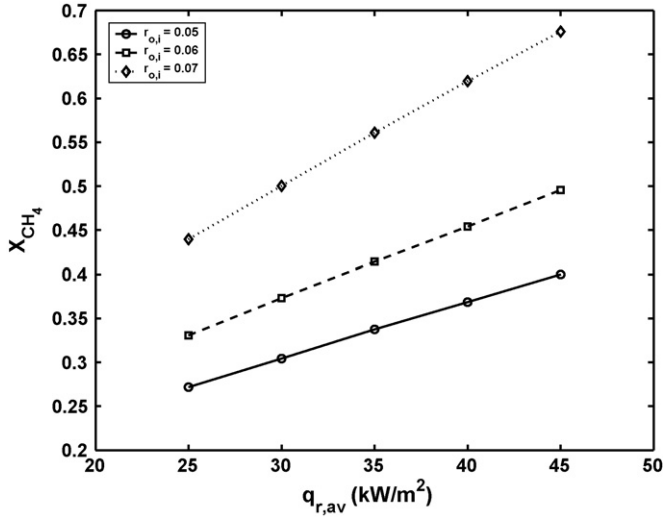

Fig. 10. Effect of the heat flux and membrane tube radius on the methane conversion.

The maximum methane conversion is obtained with the following set of values:

$$r_{o,i} = 0.07\,\text{m}, \quad F_{\text{sweep}} = 36\,\text{kmol/h}, \quad P_p = 101\,\text{kPa}, \quad A = -10\,\text{kW/m}^3$$

At these conditions, methane conversion is 0.655, carbon dioxide yield is 0.605, while Y_{H_2} is 2.243. It's worth highlighting that the conversion achieved in a traditional reactor, with the same heat amount, is just 0.400 [12]: then, an enhancement of about 63% is obtained by integrating the membrane into the reaction environment.

However, in this case, the maximum membrane temperature reached is 828.1 K, which is too high for the current Pd-based dense membranes. If a temperature limit is fixed (about 800–815 K), methane conversion is limited as well: for instance, in the same conditions shown above, but with an average heat flux equal to 30 kW/m^2, the maximum membrane temperature drops to 794 K and the methane conversion becomes 0.533.

Moreover, a steam flow rate of 36 kmol/h in the permeation zone could be a significant additional cost. Even though the retentate outlet current is burned to generate water vapour and to heat it up to 773 K and enthalpy of the permeated current is partially recovered to pre-heat up the methane feed (the heat for the reaction could be supplied by an external source, as a diathermic oil or molten salt heated by solar energy or combustion gases coming from other part of a plant), the additional methane needed to complete the steam generation and the reactant pre-heating is about 13 kmol/h. Of course, the reduction of the sweeping gas flow rate brings a lower additional methane

requirement but, at the same time, it increases the membrane temperature: therefore, a configuration is proposed with an average supplied heat flux of 30 kW/m^2 and the sweeping gas flow rate has been fixed such that no additional methane has to be burned. $F_{sweep} = 10.1$ kmol/h is obtained and the corresponding reformer performance is:

$$X_{CH_4} = 0.516 \qquad X_{CO_2} = 0.487 \qquad Y_{H_2} = 1.695$$

$$T_{mem,max} = 813.7\,K$$

Such a configuration provides a worse conversion than that of previously considered case, but it assures the following benefits:

- No additional methane is required, with economical and environmental advantages.
- The membrane temperature is lower, so its durability will be longer.

With the same total heat amount supplied to a traditional industrial reformer, the obtained conversion is 0.320: the performance improvement is about 61%, therefore, the benefit in introducing dense and selective membrane in the reactor is still strong.

Therefore, if the membrane temperature has to be limited and no additional methane cost has to be spent, this second configuration provides a more suitable solution.

4. Conclusions

A new configuration of a methane membrane reformer, similar to a shell-and-tube heat exchanger, is presented and simulated on different conditions suitable for industrial applications. A two-dimensional, non-isothermal and non-isobaric mathematical model is used in the simulations.

The effect of 4 variables (internal tube external radius, sweeping gas flow, permeation zone pressure and axial heat flux profile) is analyzed through a design matrix composed by 81 simulations. The dependences on these variables of methane conversion and membrane temperature are the main results taken into account. Possible solutions are proposed in order to satisfy different tasks, such as a methane conversion as high as possible, the compliance of the membrane thermal threshold and the zeroing of additional methane requirement for thermal reasons: the integration of membranes in reaction environment gives always strong benefits, when compared with traditional reformers.

Obviously, these benefits will be larger and larger in the future, when properly designed membranes will last for a longer time, providing also a larger permeability: so, the capability of this technology is strongly bound to the membrane performance.

Acknowledgement

This work has been carried out within the framework of the project "Pure hydrogen from natural gas through reforming up to total conversion obtained by integrating chemical reaction and membrane separation", financially supported by MIUR (FISR DM 17/12/2002).

References

[1] J. Shu, B. Grandjean, S. Kaliaguine, Methane steam reforming in asymmetric Pd and Pd–Ag porous SS membrane reactors, Appl. Catal. A Gen. 119 (1994) 305–325.
[2] Y. Lin, S. Liu, C. Chuang, Y. Chu, Effect of incipient removal of hydrogen through palladium membrane on the conversion of methane steam reforming: experimental and modeling, Catal. Today 82 (2003) 127–139.
[3] R. Gallucci, L. Paturzo, A. Basile, A simulation study of steam reforming of methane in a dense tubular membrane reactor, Int. J. Hydrogen Energy 29 (2004) 611–617.
[4] J. Oklany, K. Hou, R. Hughes, A simulative comparison of dense and microporous membrane reactors for the steam reforming of methane, Appl. Catal. A Gen. 170 (1998) 13–22.
[5] G. Madia, G. Barbieri, E. Drioli, Theoretical and experimental analysis of methane steam reforming in a membrane reactor, Can. J. Chem. Eng. 77 (1999) 698–706.
[6] W. Yu, T. Ohmori, T. Yamamoto, E. Endo, T. Nakaiwa, T. Hayakawa, N. Itoh, Simulation of a porous ceramic membrane reactor for hydrogen production, Int. J. Hydrogen Energy 30 (2005) 1071–1079.
[7] M. Chai, M. Machida, K. Eguchi, H. Arai, Promotion of hydrogen permeation on a metal-dispersed alumina membranes and its application to a membrane reactor for steam reforming, Appl. Catal. A Gen. 110 (1994) 239–250.
[8] E. Fernandez, A. Soares Jr., Methane steam reforming modeling in a palladium membrane reactor, Fuel 85 (2006) 569–573.
[9] M. Koukou, N. Papayannakos, N. Markatos, On the importance of non-ideal flow effects in the operation of industrial-scale adiabatic membrane reactors, Chem. Eng. J. 83 (2001) 95–105.
[10] A. Basile, L. Paturzo, F. Gallucci, Co-current and counter-current modes for water gas shift membrane reactor, Catal. Today 82 (1–4) (2003) 275–281.
[11] C. Fukuhara, A. Igarashi, Two-dimensional simulation of a membrane reactor for dehydrogenation of ethylbenzene, considering heat and mass transfer, J. Chem. Eng. Jpn. 36 (5) (2003) 530–539.
[12] M. De Falco, L. Di Paola, L. Marrelli, P. Nardella, Simulation of large-scale membrane reformers by a two-dimensional model, Chem. Eng. J. 128 (2007) 115–125.
[13] G. Marigliano, G. Barbieri, E. Drioli, Effect of energy transport on a palladium-based membrane reactor for methane steam reforming process, Catal. Today 67 (2001) 85–99.
[14] B. Kulkarni, L. Doraiswamy, Estimation of effective transport properties in packed bed reactors, Catal. Rev. Sci. Eng. 22 (3) (1980) 431–483.
[15] J. Xu, G. Froment, Methane steam reforming, methanation and water–gas shift: I. Intrinsic kinetics, AIChE J. 35 (1) (1989) 88–96.
[16] S. Elnashaie, S. Elshishini, Modelling, Simulation and Optimization of Industrial Fixed Bed Catalytic Reactors, Vol. 7 of Topics in Chemical Engineering, Gordon and Breach Science Publisher, 1993.
[17] E. Tsotsas, E. Schlünder, Heat transfer in packed beds with fluid flow: remarks on the meaning and the calculation of a heat transfer coefficient at the wall, Chem. Eng. Sci. 45 (1990) 819–837.
[18] A. Dixon, D. Cresswell, Theoretical prediction of effective heat transfer parameters in packed beds, AIChE J. 25 (4) (1979) 663–675.
[19] S. Yagi, D. Kunii, Studies on effective thermal conductivities in packed beds, AIChE J. 3 (3) (1957) 373–380.
[20] A. De Wasch, G. Froment, Heat transfer in packed beds, Chem. Eng. Sci. 27 (1972) 567–576.
[21] D. Kunii, J. Smith, Heat transfer characteristics of porous rocks, AIChE J. 6 (1) (1960) 71–78.
[22] M. De Falco, L. Di Paola, L. Marrelli, Heat transfer and hydrogen permeability in modeling industrial membrane reactors for methane steam reforming, Int. J. Hydrogen Energy, in press.
[23] C. Li, B. Finlayson, Heat transfer in packed beds—a re-evaluation, Chem. Eng. Sci. 32 (9) (1977) 1055–1066.

[24] M. Pedernera, J. Pina, O. Daniel, V. Bucalà, Use of a heterogeneous two-dimensional model to improve the primary steam reformer performance, Chem. Eng. J. 94 (2003) 29–40.
[25] J. Pina, N. Schbib, V. Bucalà, D. Borio, Influence of the heat-flux profiles on the operation of primary steam reformers, Ind. Eng. Chem. Res. 40 (2001) 5215–5221.
[26] I. Dybkjaer, Tubular reforming and autothermal reforming of natural gas—an overview of available processes, Fuel Process. Technol. 42 (1995) 85–107.
[27] J. Tong, Y. Matsumura, Pure hydrogen production by methane steam reforming with hydrogen-permeable membrane reactor, Catal. Today 111 (2006) 147–152.